

Ecography

**E6866**

Gifford, M. E. and Kozak, K. H. 2011. Islands in the sky or squeezed at the top? Ecological causes of elevation range limits in montane salamanders. – *Ecography* 34: xxx–xxx.

**Supplementary material**

## Supplementary material Appendix 1 – Gifford & Kozak

We modeled operative body temperatures of salamanders by solving a standard, steady state energy balance equation including terms representing solar, infra-red, convective, and conductive heat exchange,

$$Q_{\text{solar}} + Q_{\text{IRin}} = Q_{\text{IRout}} + Q_{\text{conv}} + Q_{\text{cond}}.$$

In our model of nocturnal salamander energetics, we do not consider heat generated via metabolism or lost via evaporation. In general, these salamanders live in cool wet habitats such that the contributions of metabolism and evaporation to the overall energy budget are expected to be minor (Spotila et al. 1992).

This mechanistic modeling approach proceeds by estimating the operative environmental temperature for a salamander,  $T_e$ , which is the air temperature reduced or increased by a temperature increment determined by absorbed radiation, wind speed, and animal morphology. This temperature represents the steady-state temperature of an animal with certain physical properties in a given environment. We follow the approach to modeling  $T_e$  as outlined in (Campbell and Norman 2000), and implemented in Buckley (2008), with adjustments to the radiant energy budget relevant for nocturnal forest-dwelling salamanders (see below). In order to model  $T_e$ , we must simulate the daily behavior of relevant parts of an ecosystem for a given location including, the location of the sun in the sky, daily variation in air and soil temperatures and the components of energy flux between an organism and its environment. All equations of our model are derived by Campbell and Norman (2000), unless indicated otherwise.

*Day Length and Sun Angles*

23 Salamander activity is constrained to nighttime hours. The expressions below are used  
 24 to calculate day length and time of solar noon. Solar declination, the angle between the sun's  
 25 rays and the equator:

$$26 \quad \delta = \arcsin[0.39795 \cos(0.21631 + 2 \arctan\{0.967 \tan[0.0086(-186 + J)]\})], \quad (\text{A1})$$

27 where  $J$  is the calendar day ( $J = 1$  at January 1). Thus, daylength,  $h_{day}$  (h), can be calculated  
 28 using the CBM model of Forsythe et al. (1995) as:

$$29 \quad h_{day} = 24 - \frac{24}{\pi} \arccos \left[ \frac{\sin(6\pi/180) + \sin \phi \sin \delta}{\cos \phi \cos \delta} \right], \quad (\text{A2})$$

30 where  $\phi$  is latitude (rad).

31 The time of solar noon (h) is calculated using

$$32 \quad t_0 = 12 - LC - ET, \quad (\text{A3})$$

33 where  $LC$  is the longitude correction and  $ET$  is the equation of time.  $LC$  is a correction of +1/15  
 34 hour for each degree a location is east of a standard meridian, which occur at 0, 15, 30, ...,  
 35 345°. Thus,  $ET$  is a correction for the difference between solar time and clock time, which  
 36 depends on a calendar day.  $ET$  can be calculated from

$$37 \quad ET = \frac{-104.7 \sin f + 596.2 \sin 2f + 4.3 \sin 3f - 12.7 \sin 4f - 429.3 \cos f - 2.0 \cos 2f + 19.3 \cos 3f}{3600}, \quad (\text{A4})$$

$$38 \quad f = \frac{\pi}{180} 279.575 + 0.9856J. \quad (\text{A5})$$

39 The zenith angle,  $\psi$  (rad), is the angle of the sun from vertical,

$$40 \quad \cos \psi = \sin \delta \sin \phi + \cos \delta \cos \phi \cos \frac{\pi}{12(h - t_0)}, \quad (\text{A6})$$

41 where  $h$  is hour.

42

43 *Air and Soil Temperatures*

44 Our model estimates hourly variation in air temperature,  $T_a$ , using the average maximum  
 45 and minimum daily temperatures for each month. Hourly temperature variation is modeled  
 46 using a diurnal temperature function derived by Campbell and Norman (2000):

$$47 \quad \Gamma = 0.44 - 0.46 \sin(0.9 + \omega h) + 0.11 \sin(0.9 + 2\omega h), \quad (A7)$$

48 where  $\omega = \pi/12$ . Hourly air temperature is calculated from,

$$49 \quad T_a = T_x - T_n(1 - \Gamma), \quad (A8)$$

50 where  $T_x$  and  $T_n$  are the maximum and minimum daily temperatures ( $^{\circ}\text{C}$ ), respectively.

51 We similarly model hourly soil surface temperature,  $T_s$  (K), based on mean soil  
 52 temperature and diurnal temperature range for an average day each month:

$$53 \quad T_s = T_{Sa} + A_d \sin[\omega(h - 8)], \quad (A9)$$

54 where,  $T_{Sa}$  is the average daily soil temperature (K) and  $A_d$  is the amplitude of the fluctuation in  
 55 diurnal soil temperature. In the sine function the variable for time is phase adjusted by eight  
 56 hours.

57

### 58 *Energy Flux Between an Animal and its Environment*

59 The thermal influence of radiation is dependent on the Stefan-Boltzmann law, which  
 60 describes the radiant energy over all wavelengths emitted by a blackbody radiator per unit  
 61 surface area. The result is the emitted flux density,  $B$  ( $\text{Wm}^{-2}$ ),

$$62 \quad B = \sigma(T_a + 273.15)^4, \quad (A10)$$

63 where  $\sigma$  is the Stefan-Boltzmann constant ( $5.67 \times 10^{-8} \text{ W m}^{-2} \text{ K}^{-4}$ ). The emissivity,  $\epsilon(\lambda)$ , is the  
 64 fraction of radiation emitted by a blackbody surface at a given wavelength. The emissivity of  
 65 gray bodies have no wavelength dependency. The emitted energy of a gray body,  $\Phi$  ( $\text{W m}^{-2}$ ) is,

$$66 \quad \Phi = \epsilon B. \quad (A11)$$

67 Most natural surfaces have emissivities similar to gray bodies and range from 0.95 to 1.0. We  
 68 use an emissivity value of 0.96 (Spotila et al. 1992). Clear atmosphere emissivity is  
 69 considerably lower and can be approximated using the following formula from Swinbank  
 70 (1963):

$$71 \quad \varepsilon_{ac} = 9.2 \times 10^{-6} (T_a + 273.15)^2. \quad (A12)$$

72 Convective heat transport between an animal's body and the environment depends on  
 73 wind velocity,  $u$  ( $\text{m s}^{-1}$ ) and the characteristic dimension,  $d$  (m). Assuming that wind direction  
 74 is parallel to the axis of a cylindrical approximation of a salamander,  $d$  is the animal's length  
 75 (snout-vent length [m]). Environmental turbulence is accounted for by incorporating a factor of  
 76 1.4 (Mitchell 1976). Thus, the boundary conductance of air can be expressed as

$$77 \quad g_{Ha} = 1.4 \times 0.135 \sqrt{\frac{u}{d}}. \quad (A13)$$

78 The operative wind speed (i.e., the wind speed experienced by an organism) is different  
 79 than the wind speed measured by monitoring instruments and may be attenuated by vegetative  
 80 cover (i.e., a forest canopy). Wind speed measurements are often taken 10 m above the ground.  
 81 We model the operative wind speed considering attenuation by a forest canopy by estimating  
 82 the wind speed at the bottom of the canopy and then translating this estimate to the level of a  
 83 salamander ( $\sim 5$  mm). We assume the top of canopy is 10 m high and the bottom is at  $\sim 8$  m.  
 84 The wind speed at the bottom of the canopy can be estimated by

$$85 \quad u_z = u_H \exp \left[ -LAI \left( 1 - \frac{z}{H} \right)^\beta \right], \quad (A14)$$

86 where  $u_H$  is the wind speed measured at a reference height,  $H$ ;  $LAI$  is the leaf area index; and  $z$  is  
 87 the height of the bottom of the canopy (Meyers et al. 1998). The exponent,  $\beta$ , is estimated using

88 
$$\beta = 1 - \left( \frac{\Phi - 1}{4} \right), \quad (\text{A15})$$

89 where  $\Phi$  takes a value of 2 for leafed deciduous trees.

90 The estimated wind speed at the bottom of the canopy,  $u_z$ , is then used to compute the  
91 wind speed experienced by a salamander under the canopy,  $u$ :

92 
$$u = \frac{u^*}{0.4} \ln \frac{z - d}{z_m}, \quad (\text{A16})$$

93 where  $u^*$  is the friction velocity,  $d$  is the zero plane displacement, and  $z_m$  is the momentum  
94 roughness parameter. This equation is only valid if  $z \geq d + z_m$ . The zero plane displacement is  
95 taken as  $d = 0.65h$  and the roughness parameter is  $z_m = 0.1h$ .  $h$  is the height of reference (i.e.,  
96 the salamander). The friction velocity is calculated from:

97 
$$u^* = 0.4 \left( \frac{u_z}{\ln \left( \frac{z - d}{z_m} \right)} \right). \quad (\text{A17})$$

98  
99 Radiative conductance ( $\text{mol m}^{-2} \text{s}^{-1}$ ), the thermal exchange between the animal and its  
100 environment proportional to differences in temperature is expressed as

101 
$$g_r = \frac{4\varepsilon\sigma(T_a + 273.15)^3}{c_p}, \quad (\text{A18})$$

102 where  $c_p$  is the specific heat of air ( $29.3 \text{ J mol}^{-1} \text{ K}^{-1}$ ).

103 We now calculate the radiant energy budget of an organism. Because the salamanders  
104 modeled here are nocturnal, they avoid the direct solar radiation component of the radiant  
105 energy budget (Spotila et al. 1992). Thus, our model of salamander operative temperature only  
106 considers the thermal (long-wave) component.

107 The thermal (long-wave) component of an organism's radiant energy budget is  
 108 estimated using the Stefan-Boltzmann law. This quantity is composed of the long-wave flux  
 109 densities from the atmosphere,  $L_a$ , and the ground,  $L_g$ . These flux densities are computed as

$$110 \quad L_a = \epsilon_{ac} \sigma (T_a + 273.15)^4, \quad (A19)$$

$$111 \quad L_g = \epsilon_s \sigma (T_s + 273.15)^4; \quad (A20)$$

112 where  $\epsilon_{ac}$  and  $\epsilon_s$  are the clear sky and surface emissivities, respectively.

113 Armed with these quantities we can estimate the total amount of absorbed energy as

$$114 \quad R_{abs} = \alpha_L (F_a L_a + F_g L_g), \quad (A21)$$

115 where  $\alpha_L$  is the absorptivity in the thermal waveband and  $F_a$  and  $F_g$  are the view factors  
 116 between the surface of the salamander and the thermal radiation. Because of their high water  
 117 content, salamanders are nearly perfect absorbers and emitters of thermal radiation.

118 Absorptivity ranges between 0.95 and 1.0 (Gates 1980), suggesting that a salamander will  
 119 absorb between 95 and 100% of the thermal radiation that strikes its surface. We assume a  
 120 longwave absorptance of 0.96 for our calculations (Spotila et al. 1992). We also assume that  
 121 one-half of the thermal radiation is received from both the ground and the sky as these animals  
 122 lie with the ventral surface of their body flat against the substrate and the dorsal half exposed to  
 123 the surroundings, thus  $F_a$  and  $F_g$  are both assumed to be 0.5 (following Buckley 2008). So, for a  
 124 given site, the operative environmental temperature for a salamander is calculated as

$$125 \quad T_e = T_a + \frac{R_{abs} - \epsilon_s \sigma (T_a + 273.15)^4}{c_p (g_r + g_{Ha})}. \quad (A22)$$

126

127

128

129 Table A1. Sampling localities for field abundance estimation. UTM zone for all localities is  
130 UTM17.

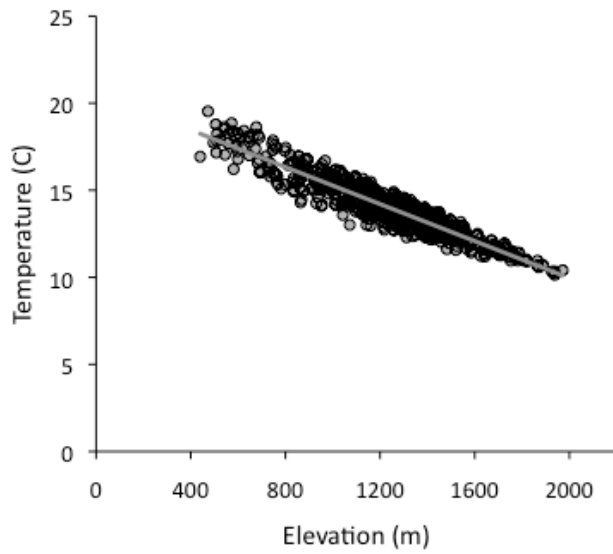
Site	Elevation (m)	Easting	Northing
1	1239	290816.90	3944136.62
2	1192	290246.58	3943395.24
3	947	288745.63	3942786.91
4	892	289177.36	3941877.60
5	774	290221.24	3939621.90
6	740	290746.19	3938033.41
7	1475	302089.70	3943018.00
8	1427	302424.40	3944294.00
9	1082	301206.80	3944879.00
10	940	299170.90	3943044.00

131

132



132 Figure A1.



133

134 Figure A1. The relationship between mean temperature and elevation are strongly correlated.

135 Temperature data represent near-ground conditions generated from the microclimate model of

136 Fridley (2009).

137

137 **Literature Cited:**

- 138 Buckley, L. B. 2008. Linking traits to energetics and population dynamics to predict lizard  
139 ranges in changing environments. *American Naturalist* 171:E1-E19.
- 140 Campbell, G., and J. Norman. 2000. *An introduction to environmental biophysics*. Springer,  
141 New York.
- 142 Forsythe, W. C., E. J. Rykiel, R. S. Stahl, H. I. Wu, and R. M. Schoolfield. 1995. A model  
143 comparison for daylength as a function of latitude and day of year. *Ecological Modeling*  
144 80:87-95.
- 145 Fridley, J. D. 2009. Downscaling climate over complex terrain: high fine-scale spatial variation  
146 of near-ground temperatures in a montane forested landscape (Great Smoky Mountains,  
147 USA). - *Journal of Applied Meteorology and Climatology* 48: 1033-1049.
- 148 Gates, D. M. 1980. *Biophysical ecology*. Springer, New York.
- 149 Meyers, T. P., P. Finkelstein, J. Clarke, T. G. Ellestad, and P. F. Sims. 1998. A multilayer  
150 model for inferring dry deposition using standard meteorological measurements. *Journal*  
151 *of Geophysical Research* 103,:22645-22661.
- 152 Mitchell, J. W. 1976. Heat transfer from spheres and other animal forms. *Biophysical Journal*  
153 16:561-569.
- 154 Spotila, J. R., M. P. O'Connor, and G. S. Bakken. 1992. Biophysics of heat and mass transfer.  
155 In *Environmental physiology of the amphibians* (eds. M. E. Feder & W. W. Burggren),  
156 pp. 59-80. Chicago: University of Chicago Press.
- 157 Swinbank, W. C. 1963. Long-wave radiation from clear skies. *Quarterly Journal of the Royal*  
158 *Meteorological Society* 89:339-348.
- 159